

BCSJ Award Article

Multi-pH Monte Carlo Simulation of Coil–Globule Transition of Weak Polyelectrolyte

Tsuyoshi Yamaguchi,* Takahiro Kiuchi, Tatsuro Matsuoka, and Shinobu Koda*

Department of Molecular Design and Engineering, Graduate School of Engineering, Nagoya University, Chikusa, Nagoya 464-8603

Received April 4, 2005; E-mail: tyama@nuce.nagoya-u.ac.jp

A generalized ensemble Monte Carlo simulation method that enables one to simulate open systems under various chemical potentials in a single run is applied to the pH titration of weak polyelectrolytes. The free energy profile has a double-minimum structure as the function of the ionization degree in poor solvents, indicating the change in the ionization degree that resembles a first-order phase transition. The two minima correspond to the less-charged globular state and the charged coil state. The structures of the polymer in the instable region of the ionization degree are investigated in detail. Results show that the conformation of the transition state consists of one blob and one or two strings. In addition to the structural inhomogeneity, a heterogeneous distribution of the charge is found there.

The generalized ensemble methods are powerful tools of computer simulation that are used in various fields including liquids, magnetism, and protein folding.[1,2] Such a method generates the artificial ensembles of states that cover a wide range of an extensive variable such as energy in a single simulation run, so as to realize the high degree of diversity of the state sampled in a run. It has the advantages over the conventional simulations in the following points. First, we can calculate the properties of the system under various conditions determined by the intensive variables such as temperature with the reweighing method.[3] Second, the escapes from the local minima that is impossible in the microcanonical or canonical simulations are enabled. Third, we can obtain the density-of-state as the function of the selected extensive variable, which is related to the entropy or the free energy of the system.

The multicanonical simulation is one of the representative examples of the generalized ensemble simulations.[4,5] The system is forced into the random walk in the energy space in the multicanonical simulation by the modification of the Boltzmann factor, so that the equal-weight sampling of the energy space is achieved. Although the originally-proposed multicanonical simulation was on the energy space, it has been extended to the spaces of other extensive variables such as magnetization,[6] volume,[7–9] and particle number.[10] In this work, we shall apply the extension of the multicanonical sampling to the particle-number space to pH titration. Since the problem we handle here is that on the system where the number of protons changes, we hereafter will refer to our novel method as "multi-pH" simulation.

The system we choose here to demonstrate our multi-pH simulation is the pH-titration of a weak polyelectrolyte in a poor solvent. The titration properties of weak polyelectrolytes (either acidic or basic) in water have been studied both experimentally and theoretically due to their industrial and engineering importance.[11] The change of the polymer conformation in correlation with the charge on the polymer has been one of the difficulties in understanding the properties of weak polyelectrolyte.

The titration curve of weak polyelectrolyte with acidic groups is usually characterized as the pH-dependence of the apparent pK_a defined as

$$pK_a \equiv pH - k_B T \log\left(\frac{\alpha}{1-\alpha}\right), \tag{1}$$

where k_B, T, and α stand for the Boltzmann constant, absolute temperature, and ionization degree, respectively. The value of pK_a is usually an increasing function of the ionization degree, which can be understood easily in terms of the electrostatic attraction between the negative charge on the polymer and the dissociating positive proton. However, in cases of a weak polyelectrolyte whose neutral state is hydrophobic, as is the case of poly(methacrylic acid) (PMA), the pK_a slightly decreases with an increase in pH in some range of the ionization degree.[11–14] Since water is a poor solvent for the neutral hydrophobic state and a good solvent for the charged state, the conformation of the chain is expected to change from the globule to the elongated coil with increasing the ionization degree. The anomaly in the pK_a has thus been ascribed to a first-order-like transition of the ionization degree associated with the coil–globule transition.[11,12]

In the last decades, there has been significant progress in the studies on the conformation of polyelectrolytes in poor sol-

Published on the web December 9, 2005; DOI 10.1246/bcsj.78.2098

vents on both the experimental and the theoretical sides. Experimentally, the development of the small angle X-ray scattering,[15–17] atomic force microscopy (AFM),[17–21] and fluorescence microscopy[22,23] has enabled us to observe the conformation of the polymer molecules in detail. Theoretically, the existence of the pearl-necklace structure was predicted based on the scaling argument,[24–26] which was confirmed by both computer simulations[26–31] and real experiments.[16–21] In contrast to the titration experiments where weak polyelectrolytes have been treated, the studies on the conformation have been performed mainly on quenched polyelectrolytes where the charged sites on a polymer are fixed, although there are some studies whose focus is placed on weak polyelectrolytes.

We consider that the titration of a weak polyelectrolyte with acidic groups in a poor solvent is a suitable system for the demonstration of multi-pH simulation for the following reasons. First, we can calculate the properties of the system under any value of pH from a single multi-pH simulation run. On the other hand, drawing the whole titration curve requires a number of grandcanonical simulation runs, since the value of pH can vary from 0 to 14 in a usual experiment, which corresponds to the change of $32k_BT$ in the chemical potential of the proton. Second, we can obtain the free energy of the system as a function of the ionization degree. Since almost all the theoretical arguments are based on the evaluation of the free energy, its direct evaluation from the simulation is valuable for the comparisons between the theory and simulation. Third, we can investigate the unstable region of the first-order-like coil–globule transition, which is impossible in the conventional grandcanonical simulation. In particular, the conformation of the transition state can be exhibited, so that we can see how the coil–globule transition proceeds.

Theoretical Formulation

Suppose that the system under simulation can exchange both the energy and particles with the external bath, which is characterized by the temperature T and the chemical potential μ. The grand canonical Boltzmann factor of the microscopic state i is given by $\exp[-(E_i - \mu N_i)/k_BT]$, where E_i and N_i are the energy and the particle number of the state i. The conventional grandcanonical simulation samples the microscopic states of the system according to this Boltzmann factor.

As is the case of multicanonical sampling in the energy space, we realize the random walk in the particle-number space by a modification of the Boltzmann factor as

$$\exp[-(E_i - \mu N_i)/k_BT] \rightarrow \exp[-(E_i - \mu N_i + k_BT \ln \Omega(N_i))/k_BT], \quad (2)$$

where the weighing factor $\Omega(N)$ is determined to achieve the uniform distribution of the ensemble in the particle-number space. The free energy of the system, $A(N;\mu)$, is related to the weighing factor as

$$A(N;\mu) = k_BT \ln \Omega(N) - \mu N. \quad (3)$$

The statistical average of a physical variable, B, under given temperature and chemical potential, denoted as $\langle B\rangle_{\mu,T}$, is determined by the following reweighing formula:

$$\langle B\rangle_{\mu,T} = \sum_N \frac{1}{\Omega(N)} e^{\frac{\mu N}{k_BT}} \langle B\rangle_{N,T}, \quad (4)$$

where $\langle B\rangle_{N,T}$ is the average of B at a given particle number and temperature.

Model

The system we consider is the spring-beads model of the linear polymer. The number of segments, denoted as N_s, is 70. We have confirmed that the characteristics of the results are the same when $N_s = 50$. Uyaver and Seidel obtained the similar titration curve to that we shall show later for the polymer of 64 segments.[32] The concentration of the polymer is infinitely dilute, and the effect of counter ions is not taken into account. Each segment takes either the protonated neutral state or the deprotonated negative one, so as to imitate the acid–base equilibrium of the weakly acidic group. The protonated and deprotonated states are different from each other solely in the charge, and the short range interactions are not affected by the protonation of the segment. The free energy required to deprotonate an isolated single segment is denoted as E_b, which is related to the bare value of pK_a as

$$pK_a^0 = \frac{2.303E_b}{k_BT}. \quad (5)$$

The value of pK_a^0 is assumed to be 5 throughout this work, which is a typical value of carboxylic acids. Since the transfer of energy and proton between the polymer and bath is allowed in the present model, the number and chemical potential of the particle described in the previous section stand for those of a proton, and the system is forced to perform the random walk along the axis of the ionization degree, $\alpha = 1 - N_p/N_s$, where N_p means the number of protonated (neutral) segments. The properties of the polyelectrolyte at a given pH are determined by the reweighing formula, Eq. 4, because pH is proportional to the chemical potential of the proton as

$$\mu_{H^+} = -2.303k_BT\mathrm{pH}. \quad (6)$$

The segments in the polymer interact with each other through the three kinds of pairwise–additive interactions as follows. The first one is the short-range van der Waals interaction in which the potential of mean force induced by the solvent is included. The functional form is given explicitly by

$$U_{ij}^{vdW}(r_{ij}) = \begin{cases} 4\varepsilon\left\{\left(\frac{\sigma}{r_{ij}}\right)^{12} - \left(\frac{\sigma}{r_{ij}}\right)^{6}\right\} + (1-h)\varepsilon & \left(r < 2^{\frac{1}{6}}\sigma\right) \\ 4\varepsilon h\left\{\left(\frac{\sigma}{r_{ij}}\right)^{12} - \left(\frac{\sigma}{r_{ij}}\right)^{6}\right\} & \left(r > 2^{\frac{1}{6}}\sigma\right) \end{cases}, \quad (7)$$

where h is the parameter that describes the "solvophobicity" of the segment. The potential described by Eq. 7 becomes the usual Lennard–Jones (LJ) one at $h = 1$, and the solvent becomes poor for the polymer due to the attractive part of the LJ potential. On the other hand, the potential becomes the repulsive part of the LJ one in the sense of Weeks, Chandler, and Andersen (WCA)[33] when h equals zero, which corresponds to the polymer in a good solvent. The simulations are performed

for $h = 0$ and 1 in this work, which are called "solvophilic" and "solvophobic," respectively. The value of ε is set equal to k_BT.

The adjacent segments are bound to each other by the finite extension nonlinear elastic (FENE) potential as

$$V_{i,i+1}^{\mathrm{FENE}}(r_{i,i+1}) = -\frac{1}{2}k_{\mathrm{FENE}}R_0^2 \ln\left(1 - \frac{r_{i,i+1}^2}{R_0^2}\right). \quad (8)$$

The spring constant k_{FENE} is set to be $30k_BT/\sigma^2$, and the maximum bond length R_0 is 1.5σ.

In addition to the short-range interactions above, deprotonated segments are interacting through the electrostatic interaction as

$$V_{ij}^{\mathrm{elec}}(r_{ij}) = \frac{k_BTl_B}{r_{ij}}. \quad (9)$$

Here, the Bjerrum length, l_B, is defined as

$$l_B = \frac{e^2}{4\pi\varepsilon_0\varepsilon_s k_BT}, \quad (10)$$

where ε_0, ε_s, and e stand for the dielectric constant of the vacuum, the relative permittivity of the solvent, and the charge of the proton, respectively. The value of l_B is fixed at 2σ throughout this work.

Computational Method

The weighing factor $\Omega(N_p)$ is determined by the iteration of short Monte Carlo simulations. Although more sophisticated and efficient algorithms for multicanonical simulations are available,[1,2] we do not employ them, merely for simplicity. The multi-pH Monte Carlo runs are performed after the convergence of the weighing factor. The length of the production run is 2×10^7 Monte Carlo steps.

Each Monte Carlo step consists of three kinds of motions. The first one is the smart Monte Carlo motion,[34] which is equivalent to the Brownian dynamics. The new configuration $\{\mathbf{r}_i^{(n)}\}$ is produced from the old one, $\{\mathbf{r}_i^{(o)}\}$, as follows:

$$\mathbf{r}_i^{(n)} = \mathbf{r}_i^{(o)} + \frac{D}{k_BT}\mathbf{F}_i + \mathbf{R}_i, \quad (11)$$

where $\mathbf{F}_i$ is the force acting on the i-th segment. $\mathbf{R}_i$ is the random number which follows the Gauss–Markov statistics and whose variation is given by

$$\langle \mathbf{R}_i \cdot \mathbf{R}_j \rangle = 6D\delta_{ij}. \quad (12)$$

The value of D/σ^2 is taken to be 0.0001.

The second kind of motion is the rotation of the dihedral angle. The dihedral angle associated with a randomly chosen bond is rotated to a random degree in order to produce the trial configuration, whose acceptance is determined by the Metropolis method.[35] Since the motions above do not accompany any change in the protonation state, they are performed in the same way as canonical simulations.

The third "motion" is the titration step. A segment is chosen by the random number, and its protonation state is altered according to the Metropolis method whose acceptance probability is determined by the generalized Boltzmann factor described in Eq. 2. The conformation of the chain and the protonation state of other segments are conserved in the titration step.

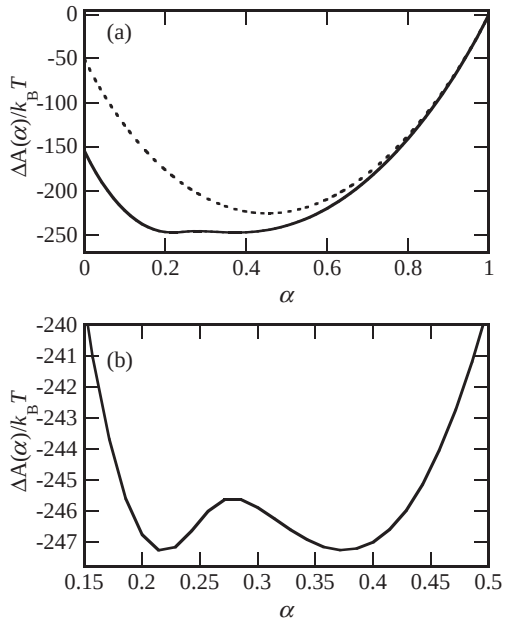

Fig. 1. The free energies of the polyelectrolytes are plotted as the function of the ionization degree, α. The difference from the free energy of the completely ionized states is shown. The solid and dotted curves are those for solvophobic and solvophilic polymers, respectively. Figure (a) exhibits the whole free energy profile, and the structure around the transition state is enlarged in Fig. (b).

Results and Discussion

Figure 1 shows the free energy of the polyelectrolytes as a function of the ionization degree. Since only the relative value of the free energy can be determined from the simulation, the difference from the completely ionized state ($\alpha = 1$) is plotted. The free energy profile at pH = 8.88 is exhibited, because the solvophobic chain ($h = 1$) experiences the coil–globule transition at this value of pH, as will be shown hereafter.

The free energy profile of the solvophilic chain ($h = 0$) is concave in the whole region of the ionization degree, which indicates that the deprotonation of the solvophilic chain occurs gradually with an increase in pH. On the other hand, the free energy profile is convex at $0.25 < \alpha < 0.30$ in the solvophobic case, which means the discontinuous change of the ionization degree that resembles to the first-order phase transition.

The transition region of the free energy profile of the solvophobic chain is enlarged in Fig. 1b, where a double-well structure is clearly demonstrated. The two minima are located at $\alpha = 0.21$ and 0.37, respectively. The ionization degree of the transition state, $\alpha = 0.27$, is close to the less-ionized minimum, and the height of the activation barrier is $1.6k_BT$. The first-order-like transition of the ionization degree of weak polyelectrolyte in a poor solvent was theoretically predicted based on the scaling argument,[26,36] and the abrupt increase of the ionization degree during the titration was exhibited in the Monte Carlo simulation study performed by Uyaver and Seidel.[32] As far as we know, however, this work is the first demonstration of the double-well structure of the free energy profile of a solvophobic weak polyelectrolyte as the function of the ionization degree.

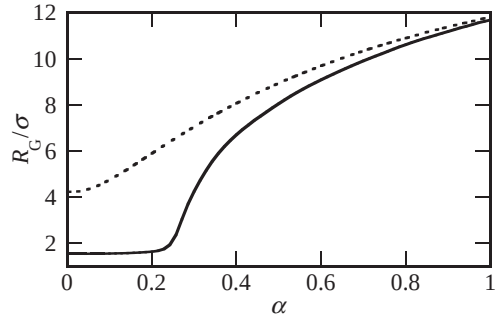

Fig. 2. The root-mean-square radius of gyration, denoted as R_G, is plotted against the ionization degree. The meanings of the symbols are the same as those in Fig. 1.

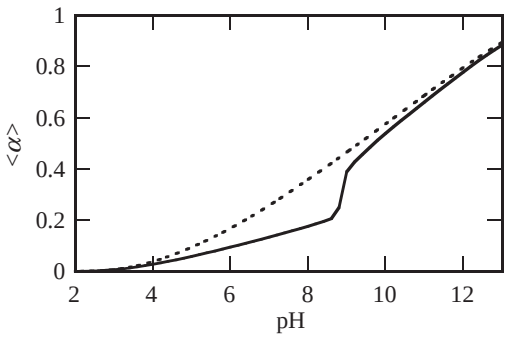

Fig. 3. The mean ionization degree, $\langle\alpha\rangle$, is plotted against pH. The meanings of the symbols are the same as those in Fig. 1.

Figure 2 shows the root-mean-square radius of gyration, denoted as R_G, as the function of ionization degree. The radius of gyration is the increasing function of the ionization degree in both the solvophilic and solvophobic cases, reflecting the Coulombic repulsion between the charged segments. The value of R_G of the solvophobic chain is smaller than that of the solvophilic one due to the short-range attractive interaction in the former case. The effect of the attractive interaction is, however, diminished for the fully charged chain, because of the dominance of the Coulombic repulsion over the short-range attraction.

The radius of gyration is a smooth function of the ionization degree in the solvophilic case. On the other hand, a sharp increase is observed around $\alpha = 0.25$ in the case of solvophobic chain. Comparing Figs. 1 and 2, one will notice that a sharp increase in the radius of gyration is observed when the first-order-like transition occurs. One may therefore safely say that the first-order-like transition of the solvophobic weak polyelectrolyte indicated in Fig. 1 accompanies the significant change in the conformation of the chain.

The mean ionization degree, $\langle\alpha\rangle$, is calculated through the reweighing method, Eq. 4, and it is plotted as a function of pH in Fig. 3. The titration curve of the polyelectrolyte in a good solvent is a smooth function of pH, as is seen in the aqueous solution of poly(acrylic acid) (PAA).[11] On the other hand, the sharp increase in $\langle\alpha\rangle$ is observed in the titration curve of the solvophobic one, as is shown in the grandcanonical simulation performed by Uyaver and Seidel.[32] The quasi-discontinuous change in the ionization degree is in harmony with the double-well structure of the free energy profile shown in Fig. 1. The transition pH and the ionization degrees at the transition are also consistent with the free energy profile. Comparing the polyelectrolytes in good and poor solvents, we find that the ionization degree of the former is larger than that of the latter, because electrostatic repulsion between the ionized segments is stronger in the latter due to its more compact conformation.

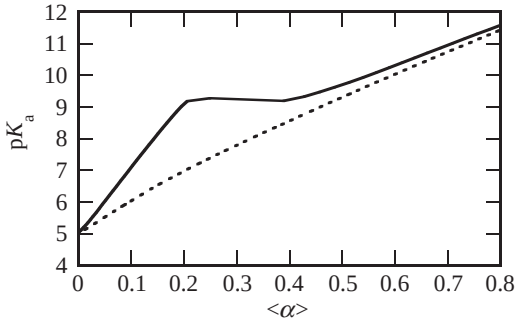

Fig. 4. The apparent pK_a, defined as Eq. 1, is plotted against the mean ionization degree. The meanings of the symbols are the same as those in Fig. 1.

The titration curves in Fig. 3 are converted into pK_a values in Fig. 4. The pK_a shows the slight decrease with the increase in the ionization degree at $0.25 < \langle\alpha\rangle < 0.40$ in the poor solvent case, as is experimentally observed in the titration of the aqueous solution of PMA. In contrast, the solvophilic chain shows the monotonic increase in pK_a, as is observed for PAA.[11]

Before going to the close investigation of the structure, we hereafter demonstrate an example of an analysis based on the free energy profile. Almost all the theoretical studies on the properties of polyelectrolyte are based on the approximate estimate of the free energy. On the other hand, the computer simulation test of the theory has been limited to the structural properties of the chain from the theory and simulation. Since the essential approximations in the theory are those on the free energy, its direct evaluation will be the crucial examination of the theory at present and in the future.

In 1990, Raphael and Joanny predicted the existence of a first-order-like transition in the titration of weak polyelectrolyte based on the scaling estimate of the free energy.[36] The solvophobic weak polyelectrolyte has the globular conformation in the less-ionized state, whose free energy is proportional to α^2. The conformation of the chain becomes rod-like when the charge density is high, and the free energy they estimated is proportional to $\alpha^{4/3}$. In the intermediate case, they assumed the cylindrical shape, and the free energy is estimated to be proportional to $\alpha^{2/3}$. The chemical potential of the charge, defined as the derivative of the free energy with respect to the charge on the chain, is a decreasing function of the ionization degree in the cylindrical conformation, which stands for the thermodynamic instability with respect to the exchange of the charge with the external bath. They therefore argued that a first-order-like transition is expected. Afterward, it was shown that the pearl-necklace structure is more stable than the cylindrical one,[24–26] and the existence of the pearl-necklace

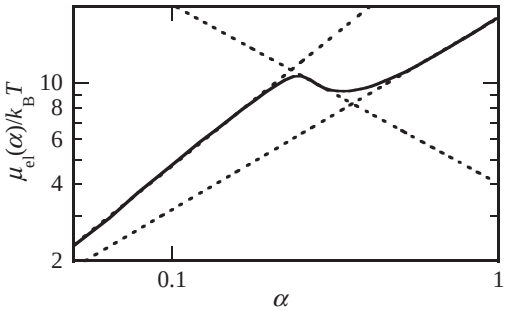

Fig. 5. The chemical potential of charge defined in Eq. 13 is plotted against the ionization degree. Only the result of the solvophobic polymer is shown as the solid curve, and it is plotted in the log–log scale. The dotted lines are the power–law fits. See text for details.

conformation has been confirmed by both computer simulations[27–31] and experiments.[16–21]

Figure 5 exhibits the chemical potential of charge, $\mu_{el}(\alpha)$, that corresponds to that estimated by Raphael and Joanny,[36] which is related to the free energy obtained in this simulation as

$$\mu_{el}(\alpha) \equiv \frac{\partial}{\partial(N_s\alpha)}[A(N_s(1-\alpha); \mathrm{pH} = \mathrm{p}K_a^0) + k_BT \ln {}_{N_s}C_{N_s}(1-\alpha)]. \quad (13)$$

The last term of Eq. 13 is related to the entropy associated with the choice of $N_p = N_s(1-\alpha)$ protonated segments among the total N_s ones, whose subtraction is necessary for the comparison with the discussion based on the strong electrolyte model. The plot is drawn in the log–log scale in order to clarify the power–law relationship. Only the result of the polyelectrolyte in a poor solvent is plotted there.

The dependence of the chemical potential of charge on the ionization degree is divided into three regions, in harmony with the prediction of Raphael and Joanny.[36] The power–law relationship holds approximately in the first and third region, as is shown in Fig. 5 as the dotted lines. Although the width of the second region is narrow, we can also apply the power–law approximation there, as is also shown in the dotted line. The exponent for the least-ionized region is 1.02, in almost perfect agreement with the theoretical one, 1.00. The exponent for the most-ionized region is 0.75, larger than the theoretical value, 1/3. The discrepancy in the exponent is also found in the intermediate region, where the simulation value is -0.70 whereas the theoretical one is $-1/3$.

The discrepancy in the intermediate region is reasonable, because the cylindrical structure theoretically assumed is not realized in the simulation, as will be shown later. However, the disagreement in the most-ionized region is not clear at present, and further studies including the system size effect will be required to make the reason clear.

Figures 6 and 7 present typical snapshots of the polymers at given ionization degrees. Figures 6 and 7 show those of the solvophilic and solvophobic ones, respectively. The conformation change of the solvophilic chain is rather simple, as is the case of the titration curve. The chain has the random coil conformation already in the neutral state. The coil extends gradually with an increase in the ionization degree, and it finally

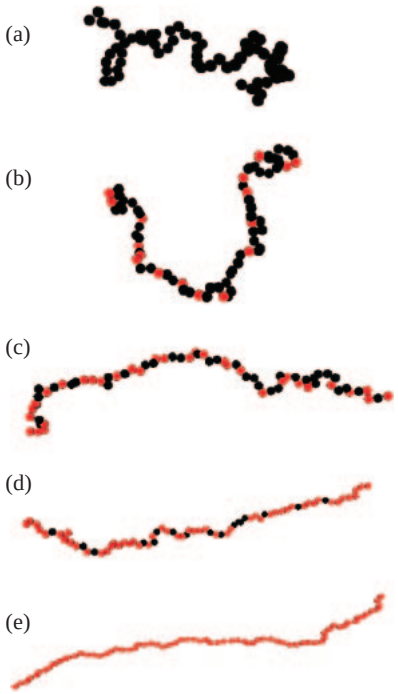

Fig. 6. The snapshots of the solvophilic chain at various ionization degrees are exhibited. The segments are shown as the sphere whose diameter is equal to σ. The red and black spheres indicate the charged and neutral segments, respectively. The ionization degrees of the chains are (a) 0.00, (b) 0.26, (c) 0.47, (d) 0.75, and (e) 1.00, respectively.

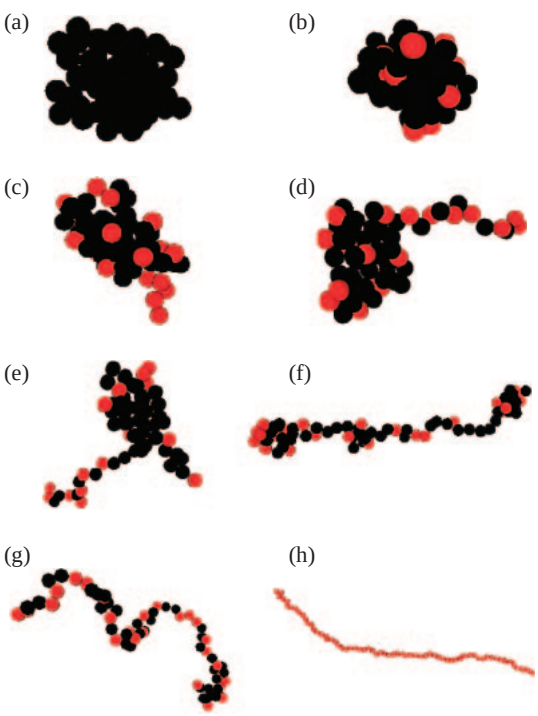

Fig. 7. The snapshots of the solvophobic chain at various ionization degrees are exhibited. The ionization degrees of the chains are (a) 0.00, (b) 0.21, (c) 0.26, (d) 0.27, (e) 0.29, (f) 0.31, (g) 0.40, and (h) 1.00, respectively. The meanings of all the symbols are the same as those in Fig. 6.

becomes the rod-like linear conformation. The distribution of charge is homogeneous compared with that of the solvophobic polymer shown below.

In contrast, the conformation of the solvophobic chain is very complicated. The conformation of the neutral chain is globule, and this is kept up to the first minimum of the free energy, $\alpha = 0.21$. The random coil structure is found in the second minimum of the free energy profile, and it is elongated to the rod-like conformation, as is the case of the solvophilic chain. Since the two minima of the free energy profile have the coil and globule character, respectively, the first-order-like transition we found in the solvophobic case belongs to the coil–globule transition.

Since the conventional grandcanonical ensemble realizes the equilibrium state of the system under the constant temperature and chemical potential, it cannot sample the thermodynamically unstable states during the coil–globule transition. However, the states between the two stable states describe the "reaction path" that tells us how the "reaction" between the coil and globule states proceeds. In particular, the characterization of the transition state is indispensable to understand the coil–globule transition as the chemical reaction. Our multi-pH simulation enables us to investigate the reaction path and the transition state of the coil–globule transition, as is demonstrated in the following paragraphs.

The transition state is close to the globule one in the axis of the ionization degree, as is already indicated in Fig. 1. The snapshots in Fig. 7 show that the transition state also has the character close to the globule state. The typical conformations around the transition state consist of one blob and one or two strings, as is exhibited in Figs. 7c–7e, and the generation of the string part is the principal barrier of the transition. The pearl-necklace structure with many blobs is found between the transition and coil states (Fig. 7f). Although the blob-string structure can be regarded as the pearl-necklace structure, the transition to the structure of one blob and one string is different from the splitting of a globule into a dumbbell proposed by Dobrynin et al.[26] We shall comment here that the intramolecular coexistence of the collapsed and coil states during the folding transition of DNA was experimentally observed by Matsuzawa et al.,[22] and it was later reproduced by the molecular simulation performed by Sakaue and Yoshikawa.[37] Since DNA is a quenched polyelectrolyte with a stiff backbone, our present result may not be applicable to DNA in a direct way, but we believe that a similar simulation method will be available for the conformational change of DNA with a proper choice of molecular models.

A close investigation of the structures of the transition state lets us notice that the ionization degree within the string part is higher than that in the whole molecule. We examine several snapshots around the transition state, and find that the ionization degree within the string is close to that of the stable coil, $\alpha = 0.4$, and that within the blob is close to the stable globule, $\alpha = 0.2$. Therefore, the blob-string structure can be regarded as the state under the intramolecular phase separation. The heterogeneous charge distribution of the pearl-necklace structure of weak polyelectrolyte was suggested by Castelnovo et al.[38] based on the perturbation treatment, and our result is in harmony with their prediction. Since the scaling argument of Dobrynin et al. is originally devised for quenched polyelectrolytes, the intramolecular heterogeneous charge distribution is not taken into account.[26] We consider it is one reason that leads to a conformation transition that is not predicted by their theory.

Summary

We propose the application of an extension of the multicanonical Monte Carlo simulation to the particle-number space to the pH titration of model weak polyelectrolytes. Our novel method, called "multi-pH" simulation, enabled us to calculate the free energy profile as the function of the ionization degree. The free energy profile of the polyelectrolyte in a poor solvent has the double-well structure, which clearly indicates that the polymer experiences a first-order-like transition during the pH titration. The two minima have the globule and coil conformations, respectively, so that the transition can be regarded as the coil–globule transition. The mean ionization degree changes almost discontinuously at the transition, and the apparent pK_a slightly decreases with the ionization degree there. These characteristics are in qualitative agreement with experiments on the aqueous solution of some hydrophobic weak polyelectrolytes.

The character of the transition state of the coil–globule transition is examined based on the snapshots. The conformation of the transition state consists of one blob and one or two strings, which is different from the splitting of the globule theoretically proposed by Dobrynin et al. for quenched polyelectrolytes.[26] The large heterogeneity of the charge distribution was also found in the transition state, which we consider is one reason for the discrepancy between the theory and simulation.

Although our present demonstration was limited to the simple model polymers, we believe it can be a powerful tool for more complicated systems such as the pH-induced denaturation of proteins.

This work was supported by Grants-in-Aid for Scientific Research on Priority Areas (No. 16041220) from the Ministry of Education, Culture, Sports, Science and Technology of Japan.

References

1 B. A. Berg, *Comput. Phys. Commun.*, **147**, 52 (2002).
2 A. Mitsutake, Y. Sugita, and Y. Okamoto, *Biopolymers*, **60**, 96 (2001).
3 A. M. Ferrenberg and R. H. Swendsen, *Phys. Rev. Lett.*, **61**, 2635 (1988).
4 B. A. Berg and T. Neuhans, *Phys. Rev. Lett.*, **68**, 9 (1992).
5 J. Lee, *Phys. Rev. Lett.*, **71**, 211 (1993).
6 B. A. Berg, U. H. Hansmann, and T. Neuhans, *Phys. Rev. B*, **47**, 497 (1996).
7 H. Okumura and Y. Okamoto, *Chem. Phys. Lett.*, **383**, 391 (2004).
8 H. Okumura and Y. Okamoto, *Phys. Rev. E*, **70**, 026702 (2004).
9 H. Okumura and Y. Okamoto, *J. Phys. Soc. Jpn.*, **73**, 3304 (2004).
10 J. R. Errington, *J. Chem. Phys.*, **118**, 9915 (2003).

11 M. Mandel, "Encyclopedia of Polymer Science and Engineering," 2nd ed, ed by H. F. Mark, N. Bikales, C. G. Overberger, G. Menges, and J. I. Kroschwitz, Wiley, New York (1988), Vol. 11.

12 M. Mandel, J. C. Leyte, and M. G. Stadhouder, *J. Phys. Chem.*, **71**, 603 (1967).

13 E. V. Anufrieva, T. M. Birshtein, T. N. Nekrasova, O. B. Ptitsyn, and T. V. Sheveleva, *J. Polym. Sci., Part C*, **16**, 3519 (1963).

14 I. Borukhov, D. Andelman, R. Borrega, M. Cloitre, L. L. Leibler, and H. Orland, *J. Phys. Chem. B*, **104**, 11027 (2000).

15 W. Essafi, F. Lafuma, and C. E. Williams, *J. Phys. II*, **5**, 1269 (1995).

16 T. A. Waigh, R. Ober, C. E. Williams, and J.-C. Galin, *Macromolecules*, **34**, 1973 (2001).

17 D. Baigl, R. Ober, D. Qu, A. Fery, and C. E. Williams, *Europhys. Lett.*, **62**, 588 (2003).

18 S. Minko, A. Kiriy, G. Gorodyska, and M. Stamm, *J. Am. Chem. Soc.*, **124**, 3218 (2002).

19 A. Kiriy, G. Gorodyska, S. Minko, W. Jaeger, P. Stepanek, and W. Stamm, *J. Am. Chem. Soc.*, **124**, 13454 (2002).

20 D. Baigl, M. Sferrazza, and C. E. Williams, *Europhys. Lett.*, **62**, 110 (2003).

21 L. J. Kirwan, G. Papastavrou, M. Borkovec, and S. H. Behrens, *Nano Lett.*, **4**, 149 (2004).

22 Y. Matsuzawa, Y. Yonezawa, and K. Yoshikawa, *Biochem. Biophys. Res. Commun.*, **225**, 796 (1995).

23 N. Miyazawa, T. Sakaue, K. Yoshikawa, and R. Zana, *J. Chem. Phys.*, **122**, 044902 (2005).

24 Y. Kantor and M. Kardar, *Europhys. Lett.*, **27**, 643 (1994).

25 Y. Kantor and M. Kardar, *Phys. Rev. E*, **51**, 1299 (1995).

26 A. V. Dobrynin, M. Rubinstein, and S. P. Obukhov, *Macromolecules*, **29**, 2974 (1996).

27 U. Micka, C. Holm, and K. Kremer, *Langmuir*, **15**, 4033 (1999).

28 P. Chodanowski and S. Stoll, *J. Chem. Phys.*, **111**, 6069 (1999).

29 H. J. Limbach and C. Holm, *J. Phys. Chem. B*, **107**, 8041 (2003).

30 S. Uyaver and C. Seidel, *J. Phys. Chem. B*, **108**, 18804 (2004).

31 S. Ulrich, A. Laguecir, and S. Stoll, *J. Chem. Phys.*, **121**, 094911 (2005).

32 S. Uyaver and C. Seidel, *Europhys. Lett.*, **64**, 536 (2003).

33 J. D. Weeks, D. Chandler, and H. C. Andersen, *J. Chem. Phys.*, **54**, 5237 (1971).

34 P. J. Rossky, J. D. Doll, and H. L. Friedman, *J. Chem. Phys.*, **69**, 4628 (1978).

35 M. P. Allen and D. J. Tildesley, "Computer Simulation of Liquids," Oxford University Press, Oxford (1987).

36 E. Raphael and J.-F. Joanny, *Europhys. Lett.*, **13**, 623 (1990).

37 T. Sakaue and K. Yoshikawa, *J. Chem. Phys.*, **117**, 6323 (2002).

38 M. Castelnovo, P. Sens, and J.-F. Joanny, *Eur. Phys. J. E*, **1**, 115 (2000).